eISSN: 2721-5717; pISSN: 2747-2124 https://journal.unhas.ac.id/index.php/zonalaut

ZONA LAUT

JOURNAL OF OCEAN SCIENCE AND TECHNOLOGY INNOVATION

A Tsunami Vulnerability Study in Ngambur and Bengkunat Districts, West Coast of Lampung Using COMCOT

Muhammad Aldhiansyah Rifqi Fauzi[1) 2)], Hani Fathul Chairiyah[2)], Ayu Libiaty Ahmad[2)], Trika Agnestasia Br Tarigan[2)3)]

[1)] Department of ICT Integrated Ocean Smart Cities Engineering, Dong-A University, Busan 49304, Republic of Korea
[2)] Department of Ocean Engineerin, Institut Teeknologi Sumatera, Lampung Selatan, 35365, Indonesia
[3)] Department of Water Resources and Environmental Engineering (WREE), Water Engineering and Management Program, Asian Institute of Technology, Pathum Thani, 12120, Thailand
Email: muhammad.fauzi@kl.itera.ac.id

Abstract

Tsunami disasters pose a significant threat to the Bengkunat and Ngambur districts in West Pesisir Regency, Lampung Province, located on the southern coast of Sumatra. Given the region's seismic activity and proximity to major fault lines, the potential for tsunamis generated by seafloor earthquakes is a critical concern. This research employs the COMCOT program to model tsunami wave propagation, run-up, arrival time, and inundation in these districts. The magnitude scenarios of 6.5, 7.5, and 8.5 were selected to reflect a range of plausible earthquake magnitudes that could impact the region. These magnitudes are relevant to real-world conditions, as evidenced by recent significant tsunami events. For instance, the 2018 Sulawesi earthquake, which had a magnitude of 7.5, resulted in devastating tsunamis and significant destruction in Central Sulawesi. The inclusion of a higher magnitude scenario (8.5) is also justified, as it aligns with the potential maximum magnitude of earthquakes that can occur in subduction zones, such as those found near Sumatra. Tsunami waves in Bengkunat and Ngambur districts showed destructive tsunami potential in each scenario. Wave height, wave inundation area and wave arrival time vary due to differences in magnitude as well as the geographical conditions of the coast and its bathymetry. The higher the magnitude, the higher the wave height and the faster the arrival time. Pagar Bukit, Suka Negara, Muara Tembulih and Sumber Agung are villages with significant damage because the wave height is above 8 m with arrival times ranging from 29-34 minutes. While Padang Dalam, Gedung Cahaya Kuningan and Parda Suka, the wave height is between 2-6 meters with a time ranging from 35-39 minutes, Inundation at magnitude 6.5 only hits the coastal area only as far as 220 meters, but at magnitude 7.5 inundation reaches about 2.4 kilometers while at magnitude 8.5 inundation reaches 3.4 kilometers. The modeling results indicate that tsunami waves in Bengkunat and Ngambur districts have destructive potential in each of the scenarios considered.

.

Keywords: COMCOT, Inundation, Tsunami

1. INTRODUCTION

The western coast of Sumatra Island is a tsunami-prone area due to its proximity to the Eurasian and Australian plates[1]. Lampung Province, adjacent to Mount Krakatoa and Anak Krakatoa, and directly bordering the Eurasian Plate to its west, is highly susceptible to tsunami disasters. According to [2], Sumatra Island has a unique geological condition characterized by two subduction zones: the first is the subduction at the boundary between the India-Australia plate and the Eurasian plate, and the second is the Sumatra Fault Zone (SFZ), also known as the Semangko Fault.

Tsunamis are formed from a series of long waves traveling towards the coast or mainland[3], caused by underwater earthquakes, landslides, volcanic eruptions, meteor impacts, and another unpredictable natural disasters, making it difficult to obtain tsunami data. Sumatra Island is one of the tsunami-prone areas in Indonesia due to frequent underwater earthquakes. Therefore, numerical modeling is a step to prevent severe damage and losses. Historically, underwater earthquakes on the west coast of Lampung in the past five years include a 5.3 SR earthquake in 2022 and a 4.8 SR earthquake in 2018. Ngambur and Bengkunat sub-districts face directly towards the Eurasian Plate and the Indian Ocean. Administratively, Bengkunat has a population

of 10,194, and Ngambur has 28,156 residents. The geographical conditions and population in these two sub-districts provide a basis for researchers to study disaster mitigation measures.
During the interval between wave propagation and wave arrival, disaster mitigation measures are critically needed to reduce both structural and physical losses. Implementing effective tsunami wave modeling based on causative factors is essential to accurately determine arrival times, run-up heights, and inundation areas. This modeling serves as foundational data for both physical and non-physical development, providing a crucial basis for comprehensive disaster preparedness and response strategies[4], [5], [6], [7].
The results of the tsunami model are highly beneficial in raising local community awareness about hazards and avoidance strategies[8]. By understanding the potential impacts of tsunami events, communities can be better prepared to respond effectively, thereby minimizing casualties and damage. Furthermore, this data supports infrastructure planning, including the strategic placement of residential areas, critical infrastructure, and designated evacuation routes.
The tsunami wave modeling program used in this research is COMCOT V.1.7, which requires seabed elevation data and earthquake parameters as model inputs. Based on the background information, this research aims to determine the wave propagation duration and tsunami wave run-up[9]. These results can be further processed using other software to obtain the inundation area. Previous tsunami modeling on the West Coast of Lampung by[10] used large grids/layers, resulting in relatively low accuracy data.

2. METHODS

The study is confined to the coordinates -4.249° to -5.742° S in Ngambur and 104.049° to 104.392° E in Bengkunat. The research focuses on 10 specific research points within this area, as illustrated in Figure 1. The data references earthquake parameters and fault by [10]. A notable earthquake in 2019 with a magnitude of 5.1 SR, located at the epicenter 7.110°S and 102.905°E, is used as a baseline. Tsunami simulations are conducted for magnitudes 6.5, 7.5, and 8.5 at the same location as the 5.1 magnitude earthquake. The earthquake orientations are detailed in Table 1.

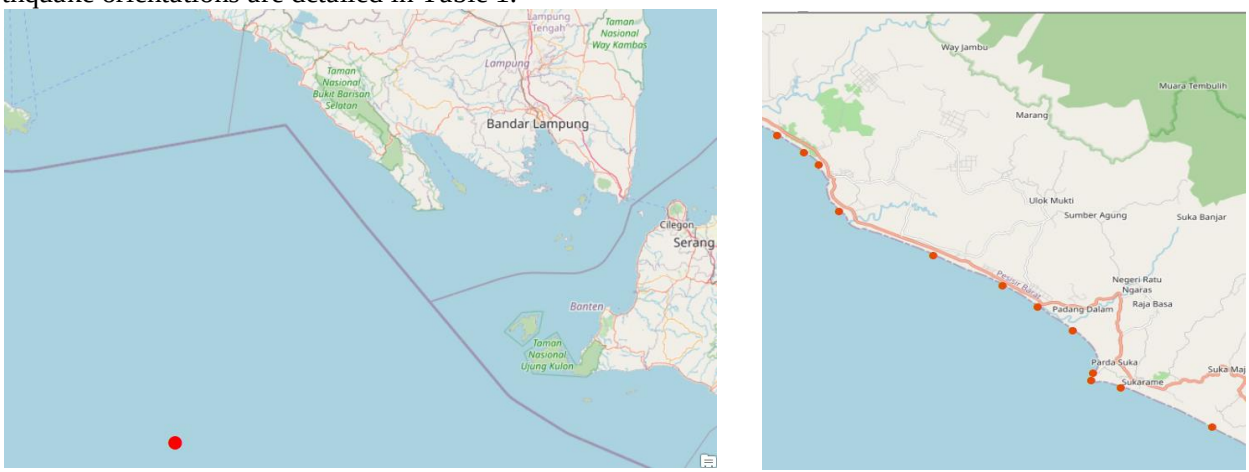

(a) (b)

Figure 1. (a) Epicenter, (b) run-up point

The simulation layers are divided into three to enhance accuracy, with grid distances of 1096 meters, 92 meters, and 15 meters. Bathymetric data for Layer 1 is sourced from the University of California San Diego (https://topex.ucsd.edu), while Layers 2 and 3 combine digitized topographic and bathymetric data from https://tanahair.indonesia.go.id. The specifics of each layer are detailed in Table 2. The simulation runs for 5400 seconds (1.5 hours) from the earthquake occurrence, recording data at 5-second intervals.

Table 1. Earthquake Parameter

Magnitude	6,5	7,5	8,5
Latitude	-7,247493°	-7,247493°	-7,247493°
Longitude	103,209845°	103,209845°	103,209845°
Fault Length	13,95	48,98	172.32
Fault Width	18,35	37,15	74,55

Magnitude	6,5	7,5	8,5
Strike	289º	289º	289º
Dip	14º	14º	14º
Rake	46º	46º	46º
Slip	28,8 meter	28,8 meter	28,8 meter
Epicenter Depth	10 Km	10 Km	10 Km

Tabel 2. Layer Resolution Data

Layer	***Latitude***	***Longitude***	***Grid Spacing***	**Grid Area (km^2)**
1	-9,316º up to -3,872º	99,025º up to 106,391º	1096 meter	493.082,03
2	-5,255º up to -5.754º	103,684º up to 104,4009º	92 meter	4.313,29
3	-4,249 º up to -5,742º	104,049º up to 104,392º	15 meter	1.717,45

In addition to earthquake parameters and bathymetric data, the roughness value or Manning's coefficient is also required for tsunami wave propagation simulations. In this study, the roughness coefficient used for the study area is based on the research Manning equation in [11]. This data is applied to Layer 3 as it encompasses terrestrial areas.

Tabel 3. Surface Roughness Index by Land Type

Land Cover Type	**Roughness Coefisient**
Water Body	0,007
Scrub	0,04
Forest	0,07
Plantation	0,035
Empty field	0,015
Agricultural	0,025
Settlement	0,045
Manggrove	0,025
Ponds	0,01

COMCOT V.1.7 employs a leap-frog numerical scheme[12]. The simulation model in this study uses nonlinear equations in spherical coordinates, incorporating bottom friction factors to depict flow motion as it propagates into shallow waters. The nonlinear equations in spherical coordinates and the bottom friction equations can be written as follows . In COMCOT, the following nonlinear shallow water equations are implemented in Cartesian coordinates as follows.

$$\frac{\partial \eta}{\partial t} + \left\{\frac{\partial P}{\partial x} + \frac{\partial Q}{\partial y}\right\} = -\frac{\partial h}{\partial t} \quad (1)$$

$$\frac{\partial P}{\partial t} + \frac{\partial}{\partial x}\left\{\frac{p^2}{H}\right\} + \frac{\partial}{\partial y}\left\{\frac{\partial Q}{H}\right\} gH\frac{\partial \eta}{\partial x} + f_x = 0 \quad (2)$$

$$\frac{\partial Q}{\partial t} + \frac{\partial}{\partial x}\left\{\frac{PQ}{H}\right\} + \frac{\partial}{\partial y}\left\{\frac{Q^2}{H}\right\} gH\frac{\partial \eta}{\partial y} + f_y = 0 \quad (3)$$

$$F_x = \frac{gn^2}{H^{\frac{7}{3}}} P(P^2 + Q^2)^{\frac{1}{2}} \quad (4)$$

$$F_x = \frac{gn^2}{H^{\frac{7}{3}}} P(P^2 + Q^2)^{\frac{1}{2}} \quad (5)$$

Where:

η	= Water elevation
$(h + ŋ)$	= Total water depth (m)
P and Q	= flux volume in x and y(m^2/s)
g	= Gravitation (m/s^2)
Fx Fy	= Friction in X and Y direction
n	= Basic friction coefficient

3. RESULTS AND DISCUSSION

3.1. Initial Conditions

Based on Figures 2 (a-c), it is evident that yellow regions indicate wave height increase/uplift, while blue regions show wave height decrease/subsidence. Higher magnitude scales result in wider fault lines. The differences among the three scenarios are also observable in the increasing length and width of the faults as the earthquake magnitude increases.

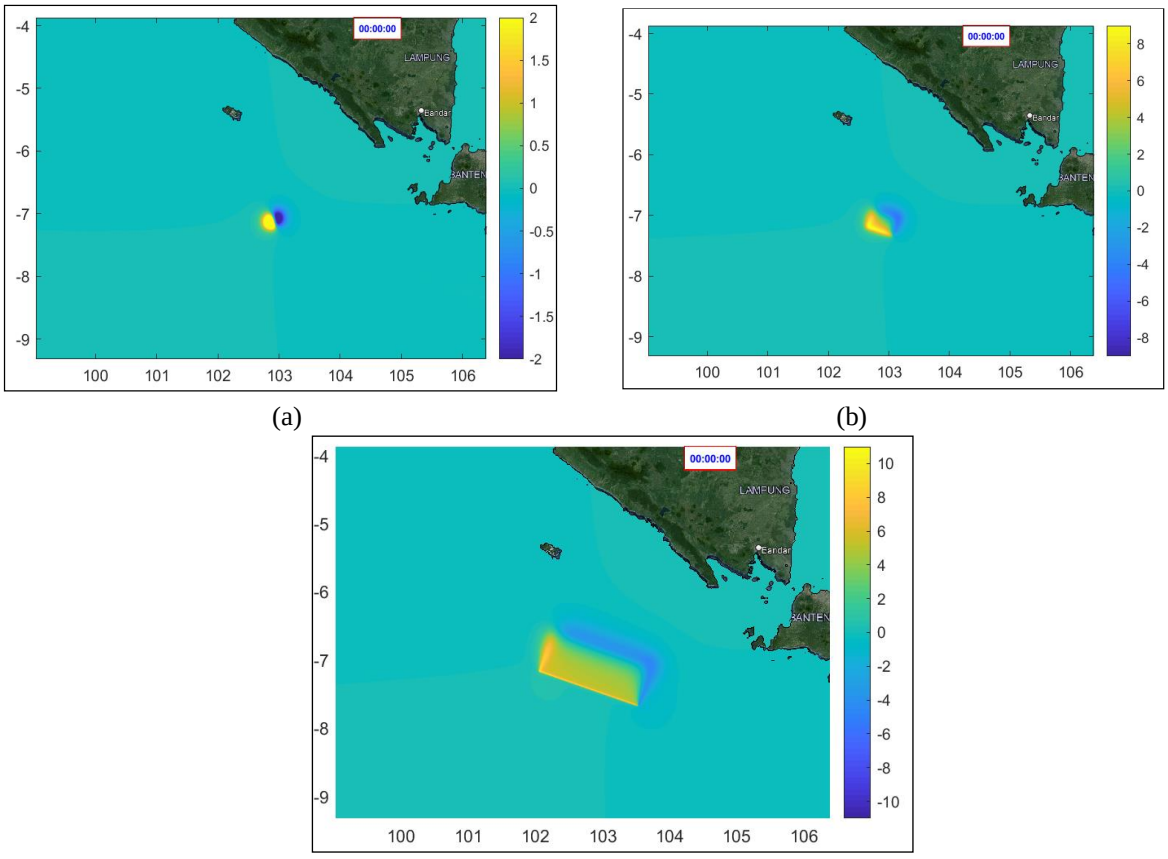

(a) (b)

(c)

Figure 2. Initial water elevation at magnitude (a) 6,5, (b) 7.5, and (c) 8,5

3.2. Wave Propagation

In the magnitude 6.5, the tsunami reaches the coastal area within 40–60 minutes figure 3 (a-c). The model results indicate that the tsunami arrival time depends on the earthquake magnitude. The waves undergo refraction, diffraction, and reflection across Enggano Island before reaching the coastline of West Coast Lampung Province. The final wave propagation at a magnitude of 6.5 indicates that the tsunami can reach coastal line and have potential destruction damage.

In the tsunami model with magnitude 7.5, tsunami waves enters Ngambur and Bengkunat districts within 30–40 minutes. The model results show the arrival time of the tsunami depends on the earthquake magnitude. The waves experience refraction, diffraction, and reflection across Enggano Island before reaching the coastline of West Coast Lampung Province. The final wave propagation at a magnitude of 7.5 indicates that the tsunami waves have higher potential damage to residential area.

Figure 5 shows the tsunami reaches Ngambur and Bengkunat districts approximately 30 minutes after the earthquake. The model results indicate that the tsunami arrival time depends on the earthquake magnitude. The waves undergo refraction, diffraction, and reflection across island before reaching the coastline of West Coast Lampung Province. The final wave propagation at a magnitude of 8.5 indicates that the tsunami is destructive to residential areas and livelihoods.

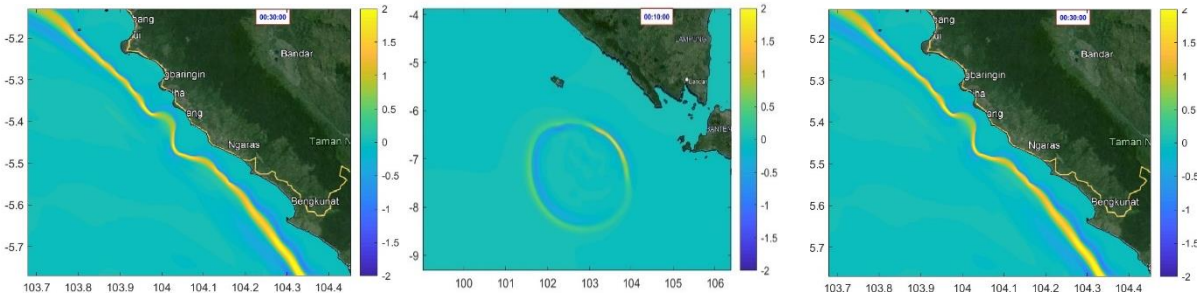

(a) (b) (c)

Figure 3. (a) = Wave propagation on magnitude 6,5 *Layer* 1 at 10th minute, (b) *Layer* 2 at 30th minute, (c) 6,5 *Layer* 3 at 40th minute,

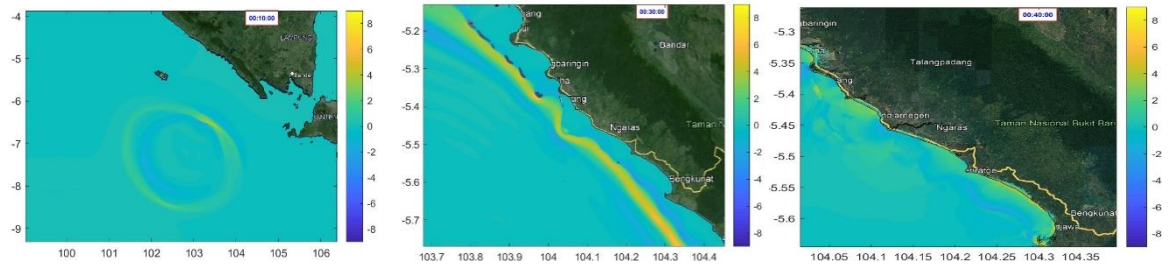

(a) (b) (c)

Figure 4. (a) = Wave propagation on magnitude 7,5 *Layer* 1 at 10th minute, (b) *Layer* 2 at 30th minute, (c) 6,5 *Layer* 3 at 40th minute,

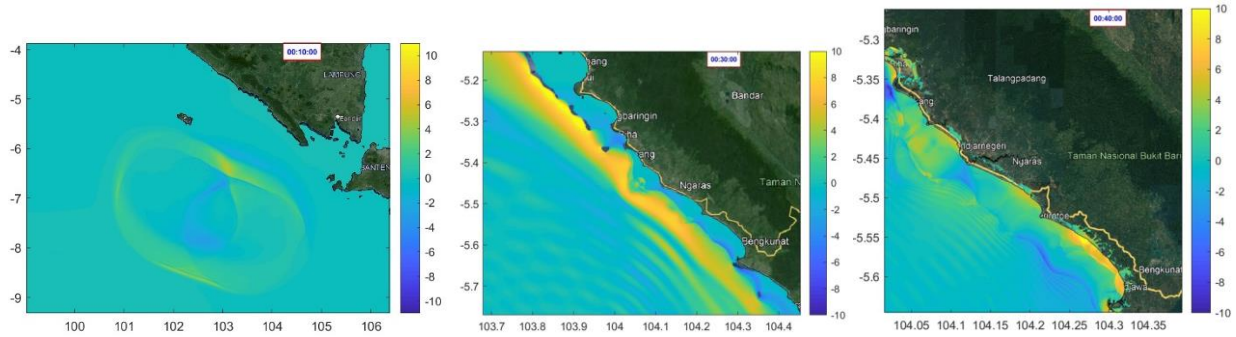

(a) (b) (c)

Figure 5. (a) = Wave propagation on magnitude 8,5 *Layer* 1 at 10th minute, (b) *Layer* 2 at 30th minute, (c) 6,5 *Layer* 3 at 40th minute,

From the wave propagation results, it can be concluded that at the 10th minute on Layer 1, the waves exhibit subsidence towards Sumatra Island and uplift towards the Indian Ocean. The coverage area will become increasingly larger due to the increasing length and width of the faults in line with the increasing magnitude scale.

3.3. Run-up and Arrival Time

The wave run-up can be observed when the tsunami wave reaches the coastline. The height and arrival time of the tsunami wave at the coastline were measured at several sample points, as detailed in Table 4.
Based on Figure 6-8, there is mareogram to show run-up height and times with At point nine, or Muara Tembulih, the arrival time is faster compared to several locations in the Bengkunat District, which are closer to the earthquake source. This discrepancy can be attributed to significant differences in the sea contour, leading to wave refraction phenomena. Additionally, before reaching Sukarame village, a headland obstructs the perpendicular wave path towards the village. In contrast, Muara Tembulih village faces directly towards the earthquake epicenter, resulting in a more direct wave impact.
This analysis underscores the importance of considering local geographical features when assessing tsunami impacts and highlights the variability in wave arrival times and heights due to these factors.

Tabel 4. Observation Location Point

Point	*Latittude*	*Longitude*	Regional Name
1	104,267	-5,550	Sukarame, Bengkunat
2	104,220	-5,529	Sukarame, Bengkunat
3	104,211	-5,526	Pantai Ujung Siging, Bengkunat
4	104,208	-5,520	Parda Suka, Bengkunat
5	104,203	-5,505	Padang Dalam, bengkunat
6	104,190	-5,494	Gd Cahaya Kuningan, Ngambur
7	104,177	-5,484	Gd Cahaya Kuningan, Ngambur
8	104,150	-5,469	Suka Negara, Ngambur
9	104,114	-5,451	Muara Tembulih, Ngambur
10	104,105	-5,430	Sumber Agung, Ngambur
11	104,101	-5,425	Sumber Agung, Ngambur
12	104,094	-5,420	Sumber Agung, Ngambur

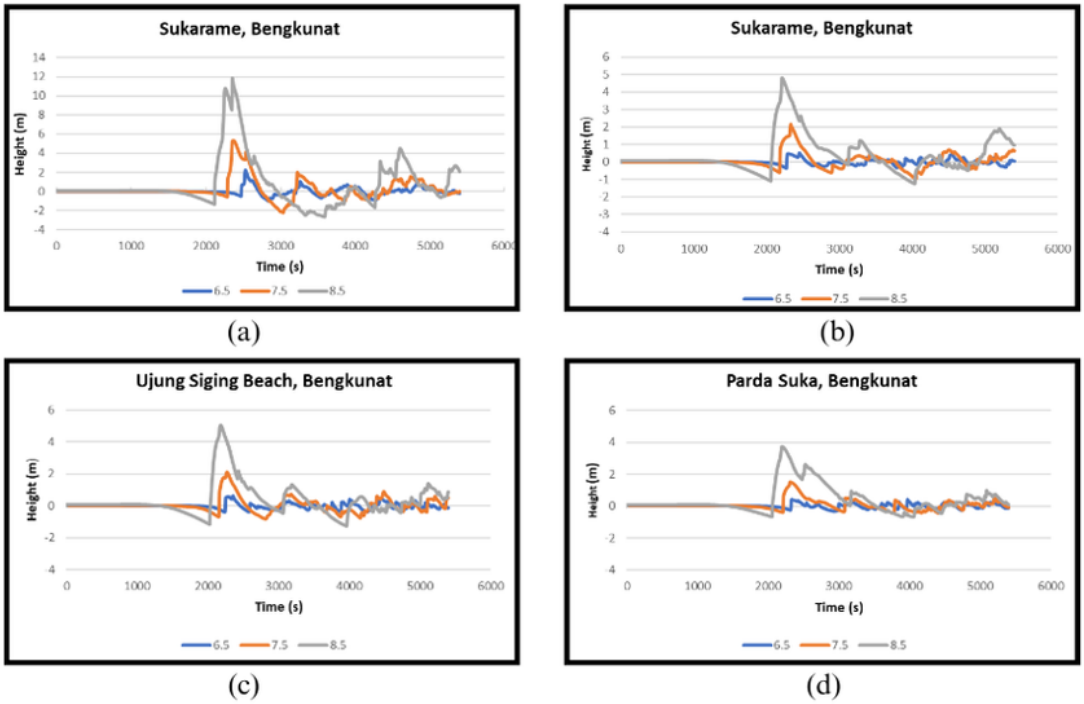

Figure 6. Mareogram in research location, (a) point 1, (b) point 2, (c) point 3, (d) point 4

Table 5 presents the run-up heights and arrival times of tsunami waves at various points for different earthquake magnitudes (6.5, 7.5, and 8.5). The run-up heights range from 0.40 meters to 11.85 meters, with higher magnitudes generally resulting in greater run-up heights. Notably, Point 1 exhibits the highest run-up height of 11.85 meters for an 8.5 magnitude earthquake. Arrival times vary across the points, with times ranging from approximately 34.3 minutes to 42.2 minutes. Point 9 shows the fastest arrival time of 34.3 minutes for an 8.5 magnitude earthquake, while Point 1 has the longest arrival time of 42.2 minutes for a 6.5 magnitude earthquake. This data highlights the variability in tsunami impacts depending on the location and earthquake magnitude, emphasizing the importance of localized assessments for effective tsunami preparedness and response.

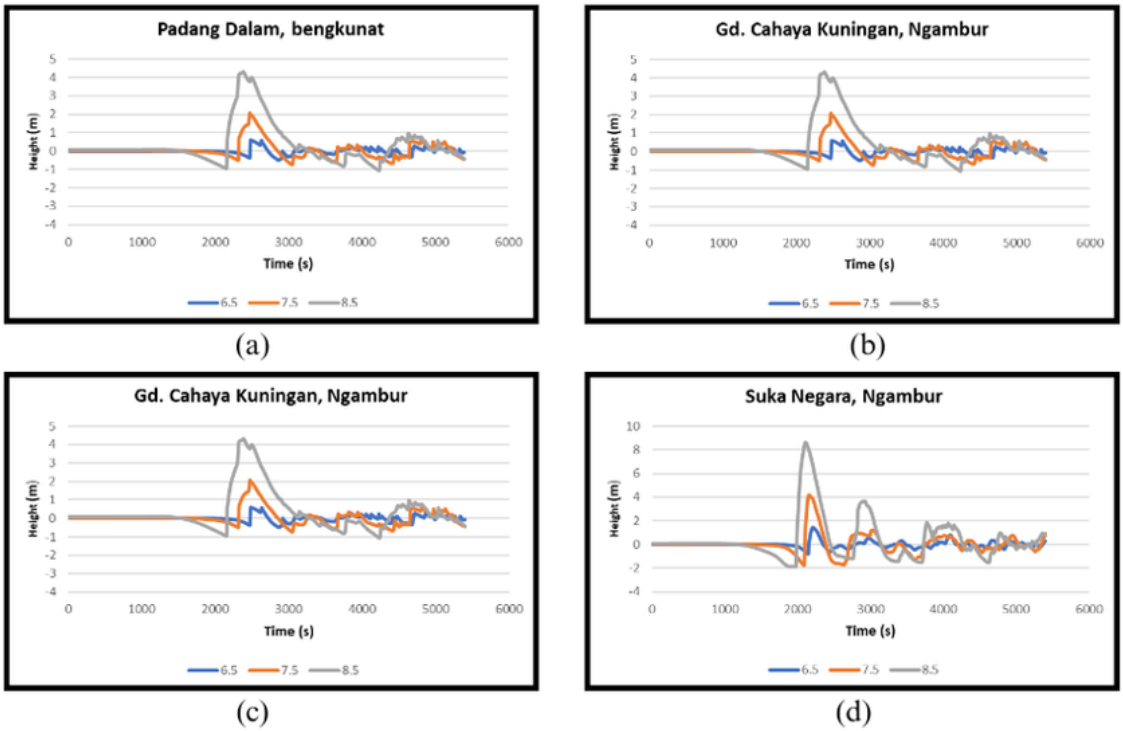

Figure 7. Mareogram di titik lokasi penelitian, dengan (a) = titik 5, (b) =t itik 6, (c) = titik 7, (d) = titik 8

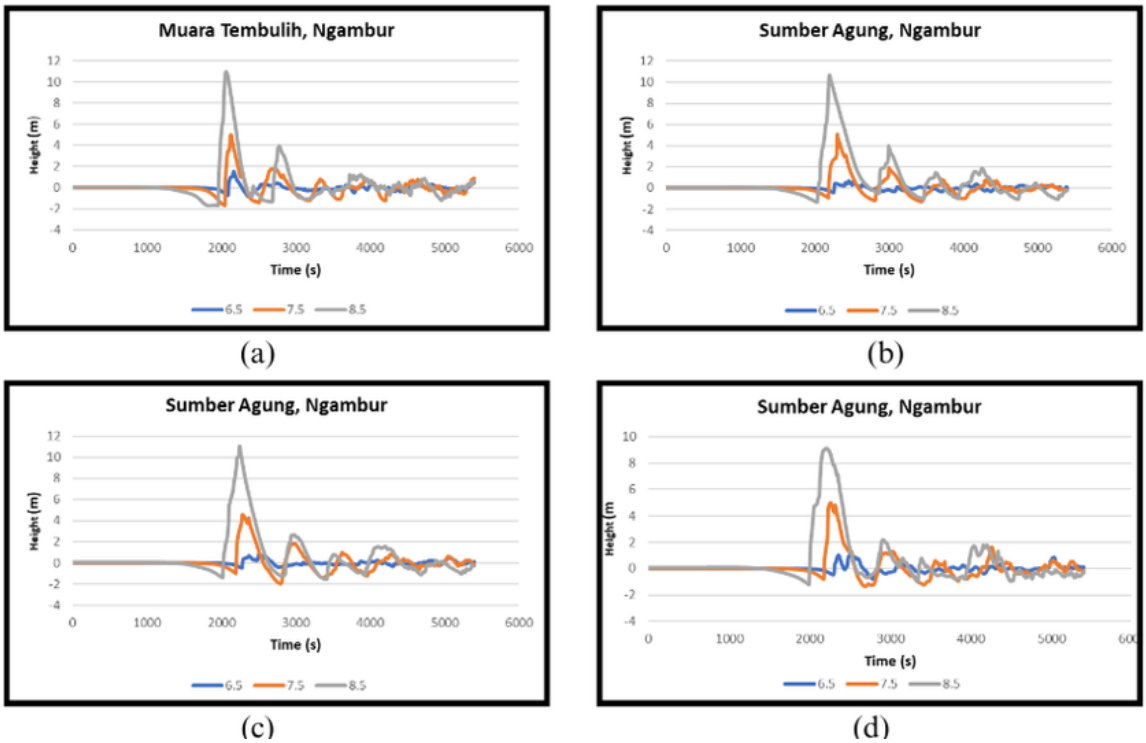

Figure 8. Mareogram di titik lokasi penelitian, dengan (a) = titik 9, (b) = titik 10, (c) = titik 11, (d) = titik 12

Table 5 Run-up Height and Arrival Time

Titik	Run-up (m)			Arrival time (min)		
	6,5	7,5	8,5	6,5	7,5	8,5
1	2.22	5.32	11.85	42,2	39,5	39,3
2	0,51	2,15	4,81	40,8	38,9	36,9
3	0,63	2,11	5,05	39,2	37,8	36,3
4	0,40	1,50	3,72	38,8	38,5	36,5
5	0,60	2,07	4,3	41,4	41,2	39,5

Titik	Run-up (m)			Arrival time (min)		
	6,5	7,5	8,5	6,5	7,5	8,5
6	0,60	2,26	5,5	40	41	39,1
7	0,40	1,80	4,34	40,3	39,9	38,1
8	1,43	4,16	8,61	36,8	35,9	35,1
9	1,54	5,01	10,95	36,1	35,5	34,3
10	0,65	5,09	10,66	41	38,5	38,1
11	0,78	4,58	11,04	41,7	38	38,1
12	1,28	5,00	9,11	`41,9	37,7	38,1

3.4. Inundation

Inundation refers to the maximum horizontal distance that tsunami waves travel inland from the shoreline. The height of the inundation decreases as the distance and area from the shoreline increase. Figures 9 to 11 below illustrate the inundation results for tsunamis with magnitudes of 6.5, 7.5, and 8.5.

One of the criteria for a tsunami to be considered destructive is if the magnitude is equal to or greater than 6.5. The coastal areas in Ngambur District and Bengkunat District are densely populated with mangroves along their shorelines, which function to reduce the energy of tsunami waves. In this study, the model results for a magnitude 6.5 tsunami show a maximum wave height of 2.22 meters occurring in Pagar Bukit Village, Ngambur District, as depicted in Figure 6. Figure 9 shows that the inundation only reaches the coast and the mangrove forest. The model results for a magnitude 7.5 scenario indicate a maximum wave height of 5.32 meters in Pagar Bukit Village, Ngambur (as seen in Figure 7), while Figure 10 shows that the maximum inundation reaches approximately 2.2 kilometers from the shoreline, affecting several settlements and facilities where residents seek natural resources. For a magnitude 8.5 scenario, the model results indicate a maximum wave height of 11.85 meters in Pagar Bukit Village, Ngambur (as seen in Figure 8), while Figure 11 shows that the inundation reaches approximately 4.34 kilometers from the shoreline.

From these results, the tsunami model simulation in this study concludes that a tsunami with a magnitude of 6.5 is destructive only to coastal areas and mangrove forests. In contrast, tsunamis with magnitudes of 7.5 and 8.5 are destructive due to the wave penetration far beyond the shoreline and the inundation height exceeding 1 meter.

Figure 9. Inundation map for magnitude 6.5

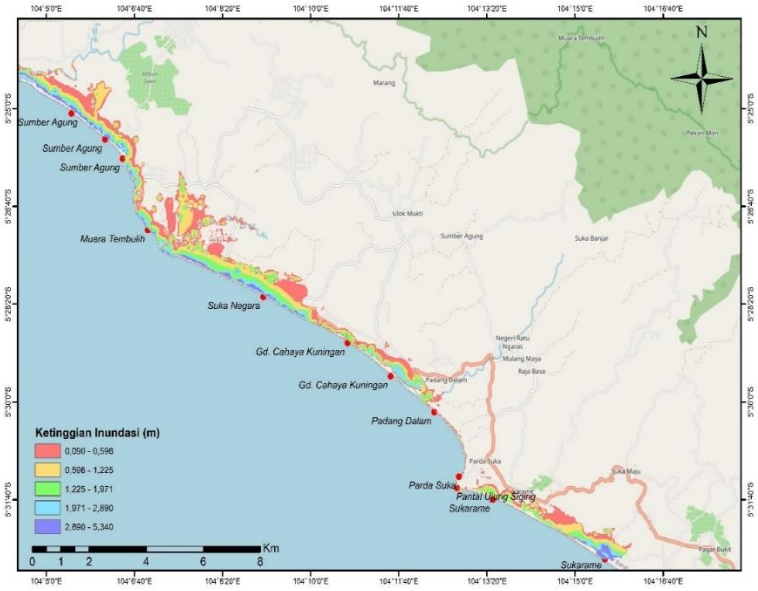

Figure 10. Inundation map for magnitude 6.5

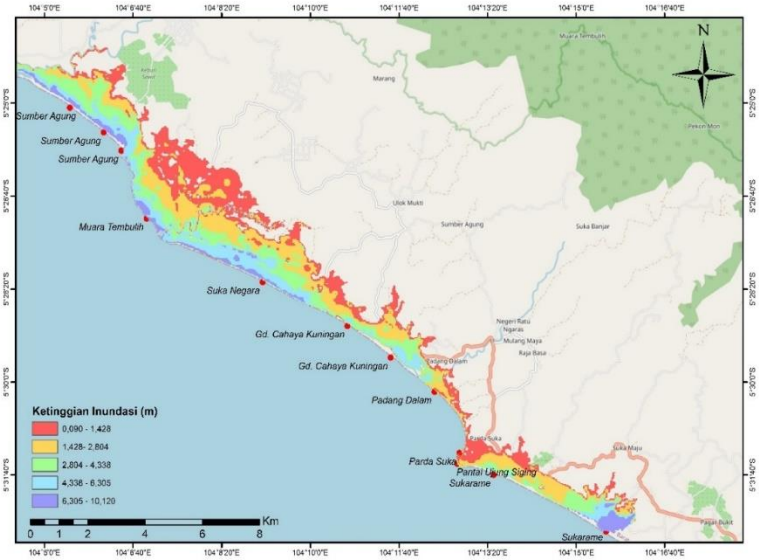

Figure 11. Inundation map for magnitude 6.5

4. CONCLUSION

In this study, the tsunami can be categorized as a local tsunami because the distance from the earthquake source to the shoreline is approximately 220 kilometers, and the arrival time is less than one hour, around 30–40 minutes. This propagation time can be influenced by several factors, including fault parameters such as strike, dip, and slip. Based on the data used, the fault parameter values are strike = 289°, dip = 14°, and rake = 46°. From the earthquake fault parameters, it is known that the strike direction of the fault plane is perpendicular to the West Coast of Lampung, causing the region to be affected by the tsunami waves more quickly. This is based on compass degree units and cardinal directions, indicating that the strike direction runs from the South-Southwest to the North-Northeast, resulting in wave propagation from the earthquake source towards the West Coast of Lampung and then spreading towards the Southeast, South, Southwest, West, Northwest, North, and Northeast.

The elevation of a surface, whether land or water, and coastal slope influence the extent of the tsunami's reach or inundation. The lower the elevation of an area, the greater the potential for it to be impacted by a tsunami, while the slope affects the distance the tsunami waves can travel inland. As shown in the wave propagation simulations with different magnitude scenarios, wave properties such as refraction, diffraction, and reflection occur due to elevation differences. Variations in seabed elevation cause differences in run-up

values and wave arrival times for each area. Table 4.2 demonstrates the differences in run-up values and wave arrival times resulting from variations in seabed elevation.
There is a pattern of relationship between run-up and wave arrival time in each magnitude scenario. Generally, there is a tendency that higher run-up results in faster wave arrival times. Differences in run-up values modeled by previous researchers are due to the placement of observation points and the grid resolution used. Based on the analysis and discussion, it can be concluded that the maximum tsunami height in the worst-case scenario occurs in Bengkunat District, with a tsunami height reaching 11.85 meters and an inundation distance of up to 1.8 kilometers. The tsunami arrival time from the earthquake source is 28–35 minutes after the earthquake. The observation points for wave arrival times are placed at the shoreline, so the information obtained from this modeling can serve as initial data for tsunami mitigation planning and rapid response actions when a potentially tsunami-generating earthquake occurs.

REFERENCES

[1] G. Ayunda, A. Ismanto, H. Hariyadi, D. N. Sugianto, and M. Helmi, "Analisis Penjalaran Run-Up Gelombang Tsunami Menggunakan Pemodelan Numerik 2D di Pesisir Kota Bengkulu," *Indonesian Journal of Oceanography*, vol. 2, no. 3, pp. 253–260, Oct. 2020, doi: 10.14710/IJOCE.V2I3.8572.

[2] H. Th. Verstappen, "Indonesian Landforms and Plate Tectonics," *Indonesian Journal on Geoscience*, vol. 5, no. 3, pp. 197–207, Sep. 2010, doi: 10.17014/IJOG.5.3.197-207.

[3] Radianta. Triatmadja, "Tsunami : kejadian, penjalaran, daya rusak, dan mitigasinya," p. 207, 2011.

[4] E. Pradjoko, A. Setiawan, L. Wardani, and Hartana, "The impact of mandalika tourism area development on the Kuta village, centre Lombok, Indonesia based on tsunami hazard analysis point of view," *IOP Conf Ser Earth Environ Sci*, vol. 708, no. 1, p. 012010, Apr. 2021, doi: 10.1088/1755-1315/708/1/012010.

[5] F. Kurniawan, S. Widodo, and L. Halengkara, "Pemodelan Tsunami Dan Alternatif Jalur Evakuasi Berbasis Sig Di Kecamatan Krui Selatan Tahun 2019," *Jurnal Penelitian Geografi*, vol. 10, no. 1, pp. 43–52, Mar. 2022, Accessed: Oct. 17, 2024. [Online]. Available: https://jurnal.fkip.unila.ac.id/index.php/JPG/article/viewFile/20567/15212

[6] Q. Zahro, "Spatial Study Of Tsunami Risk In Serang, Banten Kajian Spasial Risiko Bencana Tsunami Kabupaten Serang, Banten," *Jurnal Sains dan Teknologi Mitigasi Bencana*, vol. 12, no. 1, 2017.

[7] T. Mikami, T. Shibayama, M. Esteban, and R. Aránguiz, "Comparative Analysis of Triggers for Evacuation during Recent Tsunami Events," *Nat Hazards Rev*, vol. 21, no. 3, p. 04020022, Apr. 2020, doi: 10.1061/(ASCE)NH.1527-6996.0000386.

[8] Benazir, "Pengembangan Metode Simulasi Run-Up Tsunami Dan Aplikasinya Pada Beberapa Kasus Tsunami Di Indonesia," Dissertation, Universitas Gadjah Mada, 2018. Accessed: Oct. 17, 2024. [Online]. Available: https://etd.repository.ugm.ac.id/penelitian/detail/161955

[9] Z. Qonita, S. Karima, A. Rusdiansyah, and R. Riyandari, "Numerical Modeling Of The 1998 Papua New Guinea Tsunami Using The Comcot," *Barekeng: Jurnal Ilmu Matematika dan Terapan*, vol. 18, no. 1, pp. 0349–0360, Mar. 2024, doi: 10.30598/BAREKENGVOL18ISS1PP0349-0360.

[10] D. Pratiwi and D. A. Fitri, "Analisis Potensial Penjalaran Gelombang Tsunami di Pesisir Barat Lampung, Indonesia," *Jurnal Teknik Sipil Institut Teknologi Padang*, vol. 8, no. 1, pp. 5–5, Jan. 2021, doi: 10.21063/JTS.2021.V801.05.

[11] J. G. Hills and C. L. Mader, "Tsunami Produced by the Impacts of Small Asteroids," *Ann N Y Acad Sci*, vol. 822, no. 1, pp. 381–394, May 1997, doi: 10.1111/J.1749-6632.1997.TB48352.X.

[12] X. Wang, *USER MANUAL FOR COMCOT VERSION 1.7 (FIRST DRAFT)*. 2009.